

# **SnS<sub>2</sub>/Covalent Organic Frameworks S-scheme Heterostructures for Photocatalytic Water Splitting: Insights from Ground-state Properties and Nonadiabatic Excited-state Dynamics**

Yue Tang <sup>a</sup>, YiPeng Wang <sup>b</sup>, Xinlu Cheng <sup>a,\*</sup>, Hong Zhang <sup>c</sup>

<sup>a</sup> Institute of Atomic and Molecular Physics, Sichuan University, Chengdu 610065, China.

<sup>b</sup> College of Applied Technology, Shenzhen University, Shenzhen 518061, China.

<sup>c</sup> College of Physics, Sichuan University, Chengdu 610064, China.

## **List of Method, Tables and Figures**

Method.....	S1
Table S1.....	S2
Fig. S1.....	S2
Fig. S2.....	S3
Fig. S3.....	S4
Fig. S4.....	S5
Fig. S5.....	S5
Fig. S6.....	S6
Fig. S7.....	S6
Fig. S8.....	S7
Fig. S9.....	S8
Fig. S10.....	S8
Fig. S11.....	S9

## Method

The solar-to-hydrogen (STH) efficiency  $\eta_{\text{STH}}$  is calculated with the formula:<sup>1</sup>

$$\eta_{\text{STH}} = \eta_{\text{ads}} \times \eta_{\text{cu}} \quad (1)$$

where  $\eta_{\text{ads}}$  and  $\eta_{\text{cu}}$  are the efficiencies of light absorption and carrier utilization obtained using following formulas:

$$\eta_{\text{ads}} = \frac{\int_{E_g}^{\infty} P(\hbar\omega) d(\hbar\omega)}{\int_0^{\infty} P(\hbar\omega) d(\hbar\omega)} \quad (2)$$

$$\eta_{\text{cu}} = \frac{\Delta G \int_E^{\infty} \frac{P(\hbar\omega)}{\hbar\omega} d(\hbar\omega)}{\int_{E_g}^{\infty} P(\hbar\omega) d(\hbar\omega)} \quad (3)$$

where  $P(\hbar\omega)$  is the AM1.5 solar energy flux at the photon energy  $\hbar\omega$ .  $\Delta G$  is the potential difference of water splitting,  $\Delta G = 1.23$  eV.  $E$  is the minimum photon energy used for water splitting reaction and is defined as:<sup>1</sup>

$$E = \begin{cases} E_g, & (\chi(H_2) > 0.2, \chi(O_2) \geq 0.6) \\ E_g + 0.2 - \chi(H_2), & (\chi(H_2) < 0.2, \chi(O_2) \geq 0.6) \\ E_g + 0.6 - \chi(O_2), & (\chi(H_2) \geq 0.2, \chi(O_2) < 0.6) \\ E_g + 0.8 - \chi(H_2) - \chi(O_2), & (\chi(H_2) < 0.2, \chi(O_2) < 0.6) \end{cases} \quad (4)$$

where  $\chi(H_2)$  and  $\chi(O_2)$  are the overpotentials of HER and OER, respectively. Considering the effect of intrinsic electric field the STH efficiency is further corrected using the following equation:<sup>2,3</sup>

$$\eta'_{\text{STH}} = \eta_{\text{STH}} \times \frac{\int_0^{\infty} P(\hbar\omega) d(\hbar\omega)}{\int_0^{\infty} P(\hbar\omega) d(\hbar\omega) + \Delta\varphi \int_{E_g}^{\infty} \frac{P(\hbar\omega)}{\hbar\omega} d(\hbar\omega)} \quad (5)$$

**Table S1.** Corrected solar-to-hydrogen efficiencies ( $\eta'_{\text{STH}}$ ) of SnS<sub>2</sub>/COF2 and SnS<sub>2</sub>/COF3 under various strains.

Strain (%)	$\eta'_{\text{STH}} (\%)$	
	SnS <sub>2</sub> /COF2	SnS <sub>2</sub> /COF3
-6%	-	54.97
-4%	-	54.28
-2%	54.50	53.93
0%	53.64	54.19
2%	54.33	54.08
4%	54.56	54.53
6%	54.20	53.79
8%	53.20	53.92
10%	-	54.14

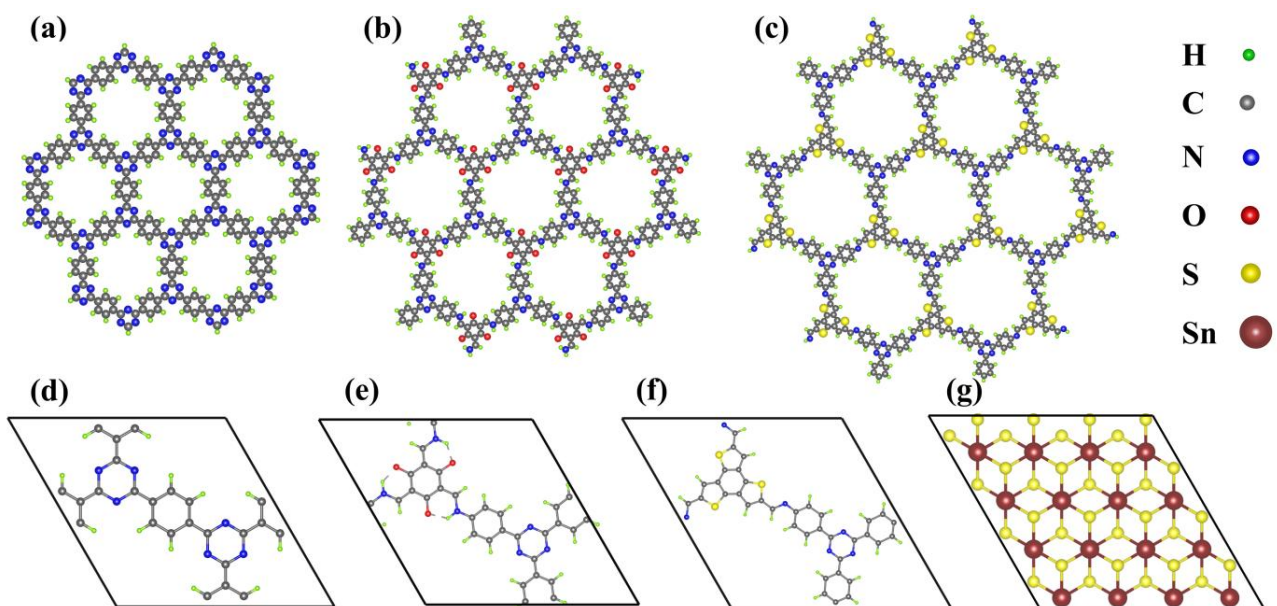


**Fig. S1** Schematic illustrations of porous covalent organic frameworks (a) COF1, (b) COF2, and (c) COF3. Top views of unit cells (d) COF1, (e) COF2, (f) COF3. (g) 4×4×1 SnS<sub>2</sub> supercell.

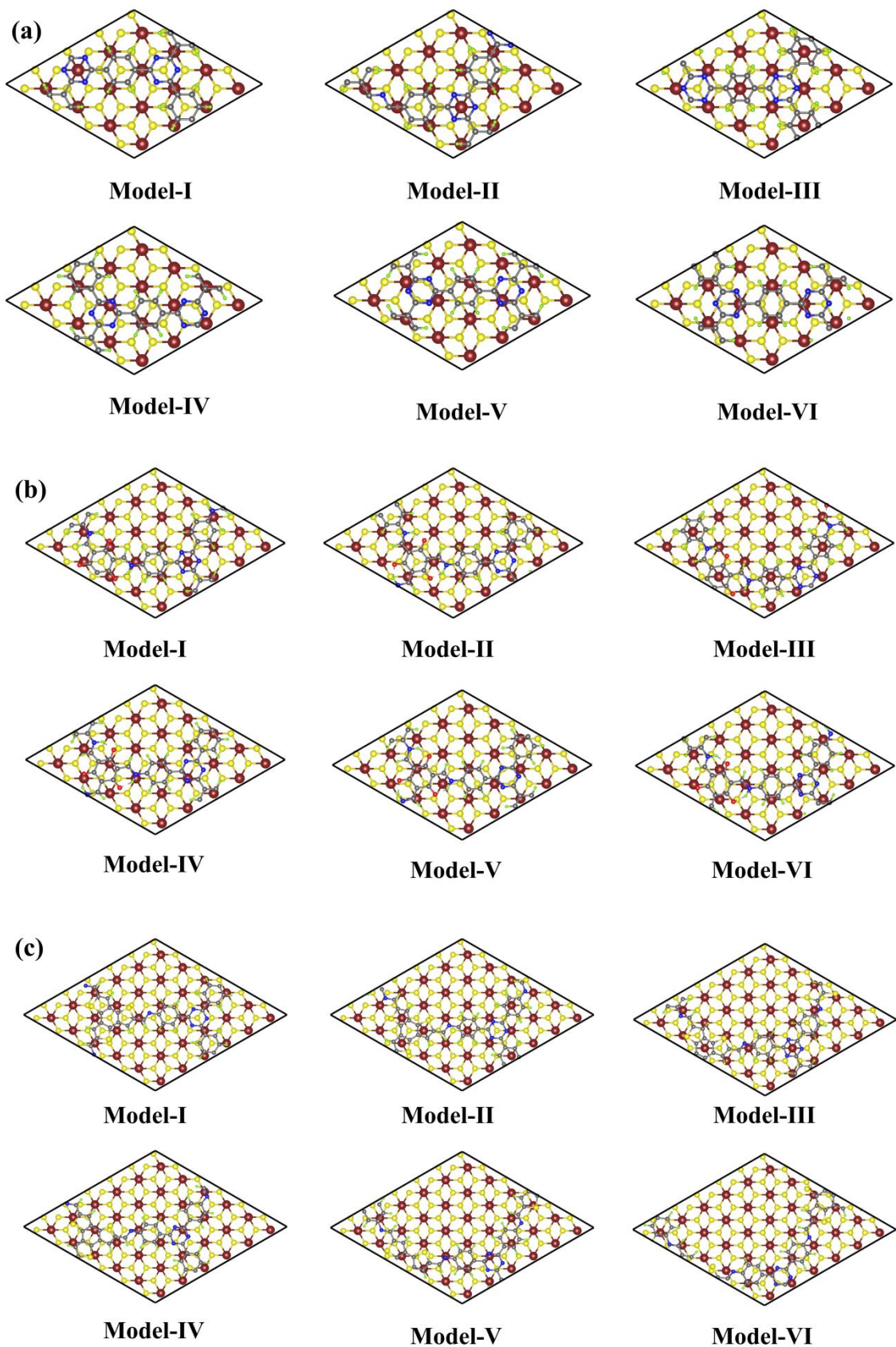


**Fig. S2** Stacking models of (a) SnS<sub>2</sub>/COF1, (b) SnS<sub>2</sub>/COF2, and (c) SnS<sub>2</sub>/COF3.

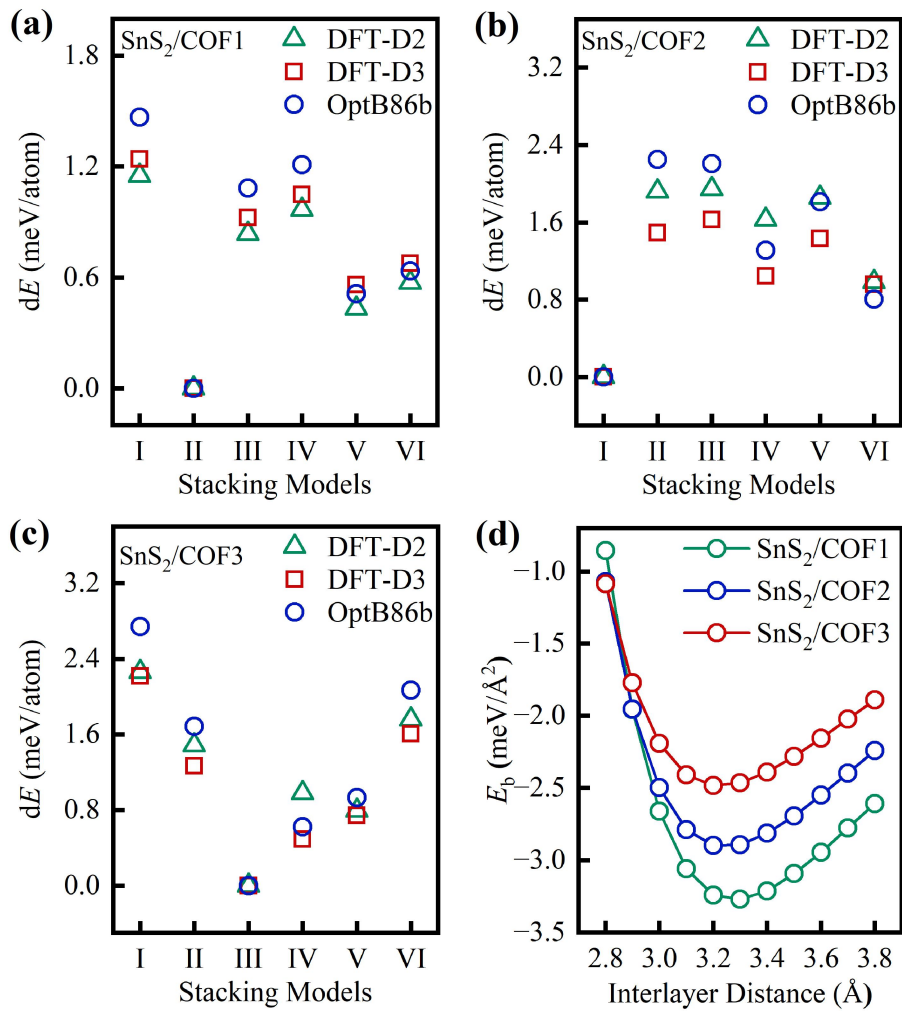


**Fig. S3** (a-c) Relative total energies of different stacking models. (d) Binding energies of  $\text{SnS}_2/\text{COFs}$  with different interlayer distance.

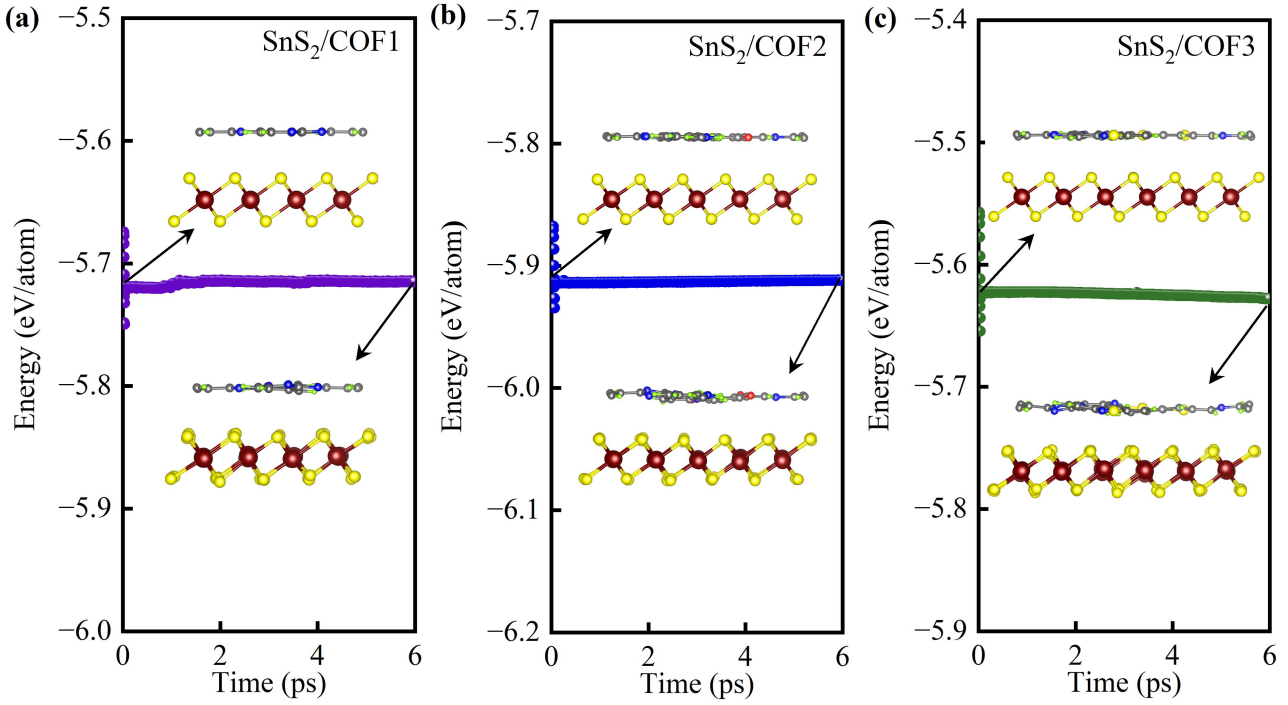


**Fig. S4** AIMD simulation results at 300 K. Insets are side views of  $\text{SnS}_2/\text{COFs}$  before and after simulations.

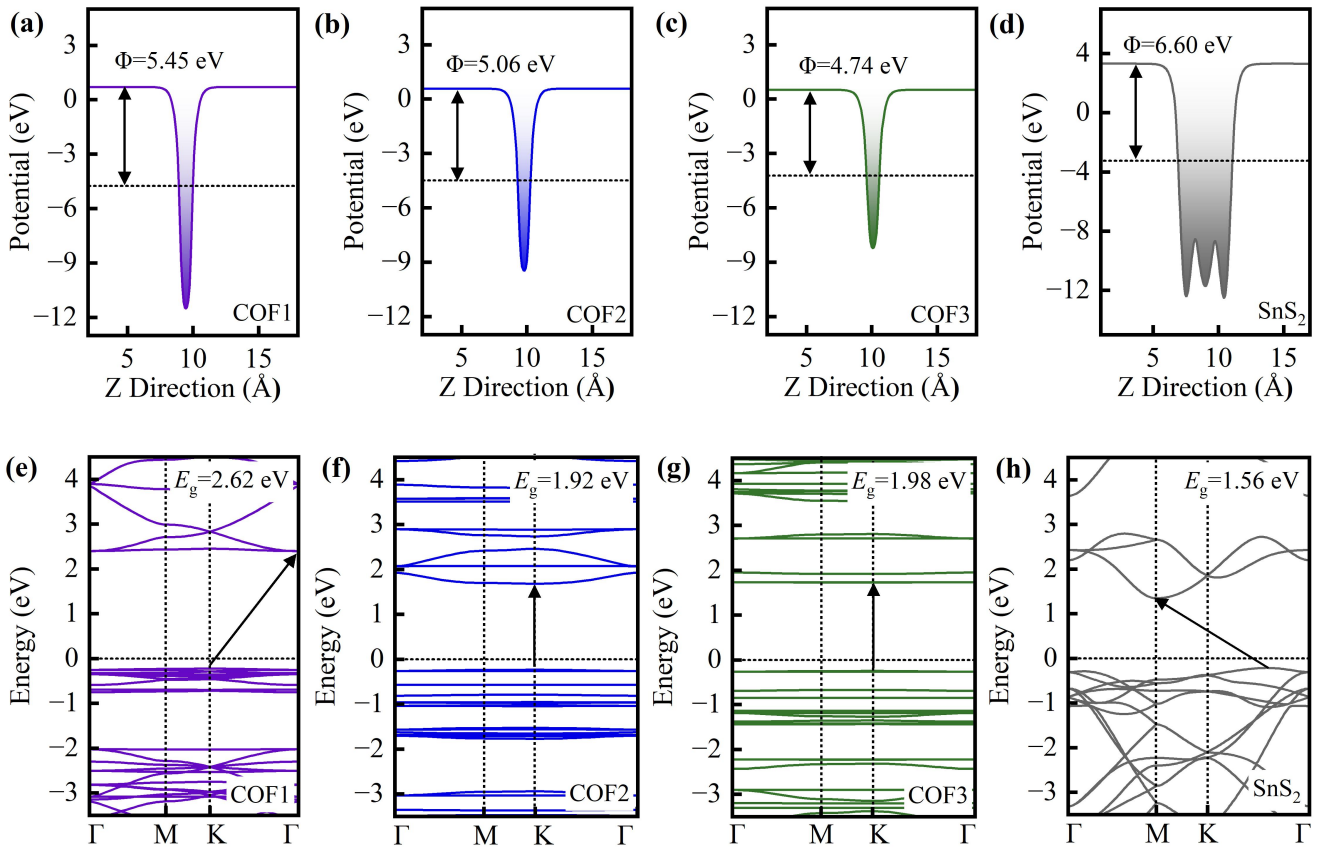


**Fig. S5** Average electrostatic potentials of (a) COF1, (b) COF2, (c) COF3, and (d)  $\text{SnS}_2$  monolayers. Dashed lines represent the Fermi levels. Band structures of (e) COF1, (f) COF2, (g) COF3, and (h)  $\text{SnS}_2$  monolayers. Arrows indicate the positions of VBM and CBM.

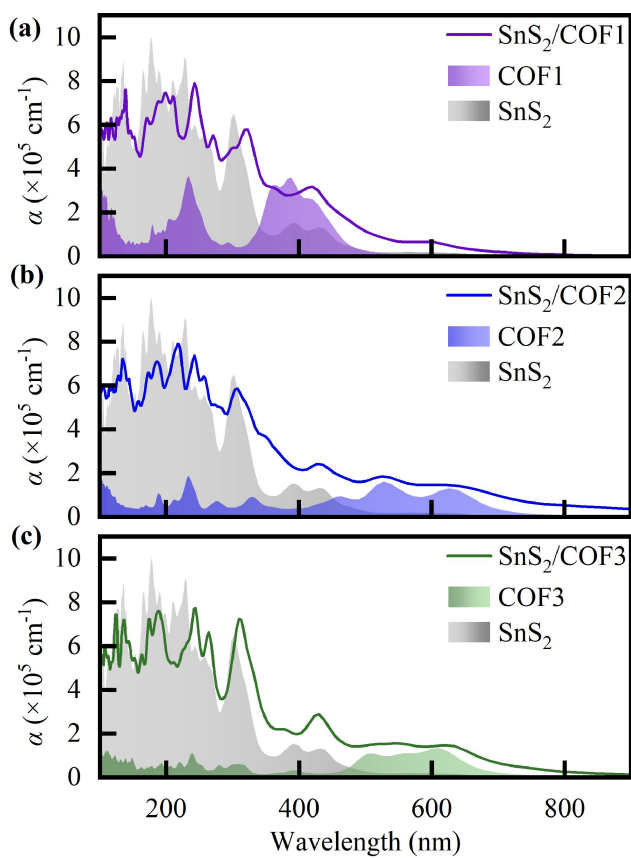


**Fig. S6** Light absorption spectrum. (a) SnS<sub>2</sub>/COF1, (b) SnS<sub>2</sub>/COF2, and (c) SnS<sub>2</sub>/COF3.

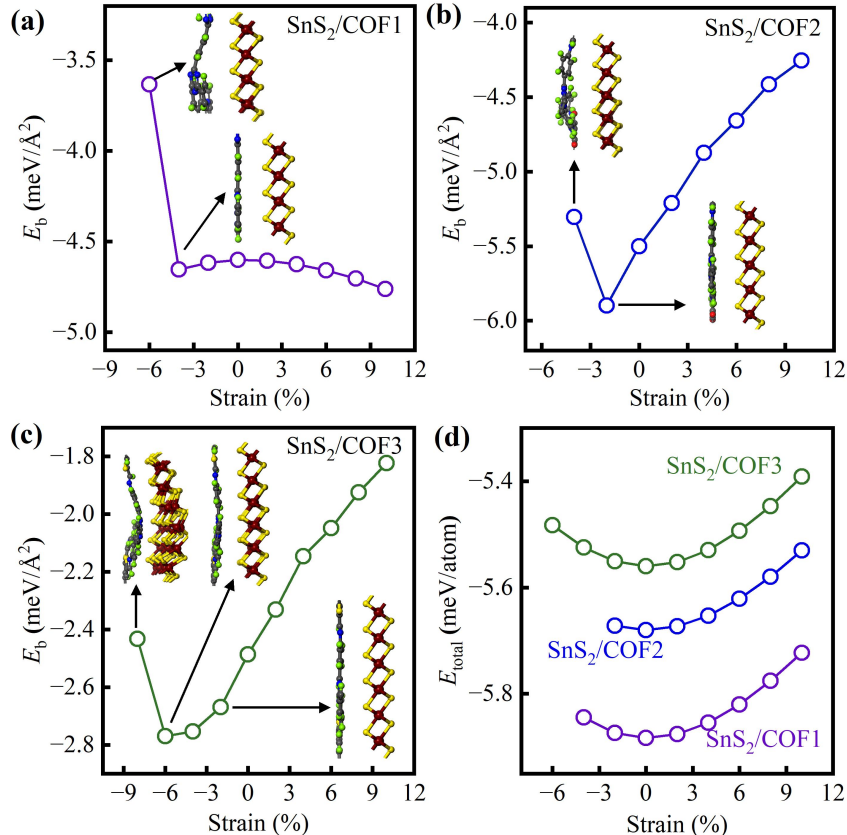


**Fig. S7** (a-c) Binding energies of SnS<sub>2</sub>/COFs as function of strain. (d) Total energies of SnS<sub>2</sub>/COFs as a function of strain.

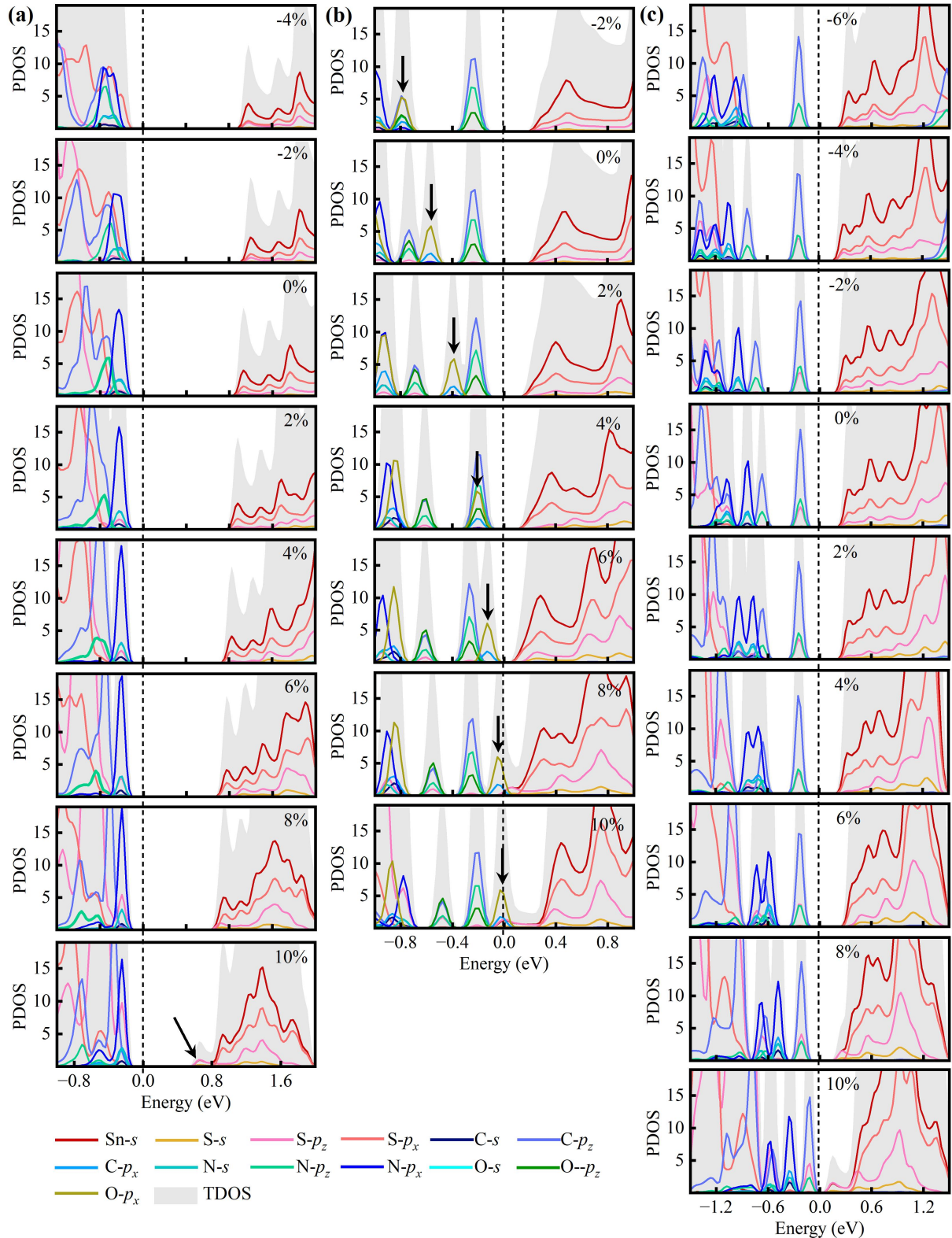


**Fig. S8** Orbital decomposed density of state of (a) SnS<sub>2</sub>/COF1, (b) SnS<sub>2</sub>/COF2, and (c) SnS<sub>2</sub>/COF3 under different strains. Gray regions represent total density of state, Lines with different colors represent different orbitals from different elements. Dashed lines represent the Fermi levels.

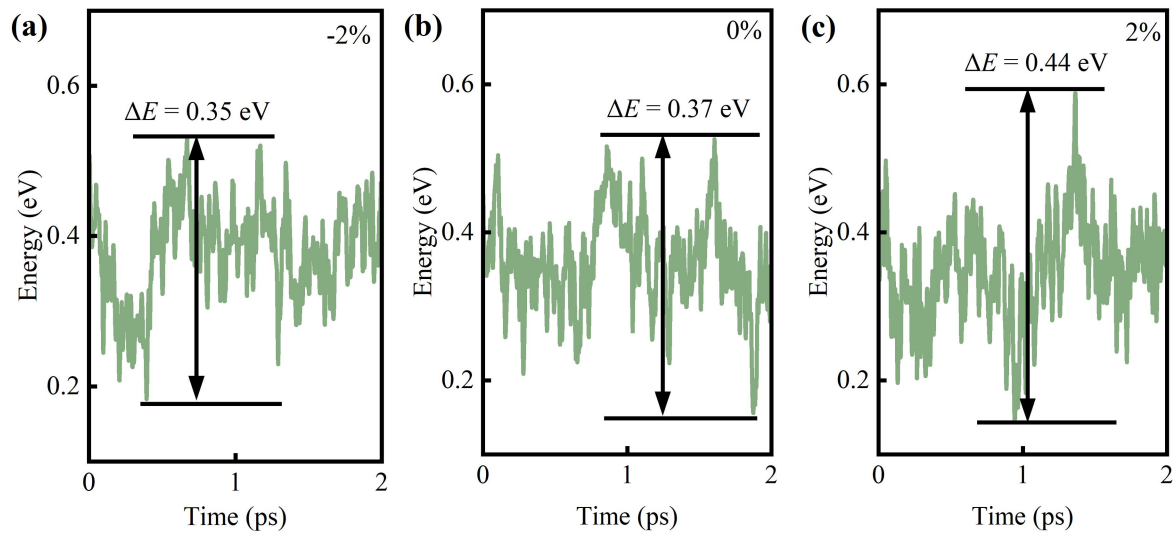


**Fig. S9** The time-dependent bang gap fluctuation in SnS<sub>2</sub>/COF3 under strain (a) -2%, (b) 0%, and (c) 2%.

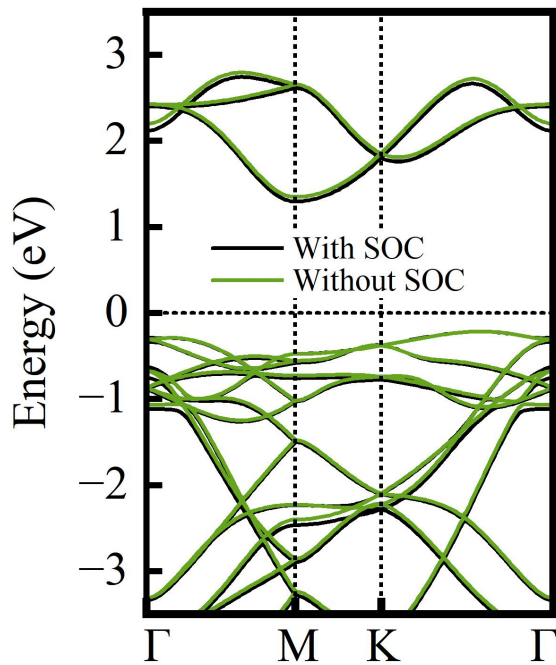


**Fig. S10** Band structures of SnS<sub>2</sub> with and without consideration of SOC effect.

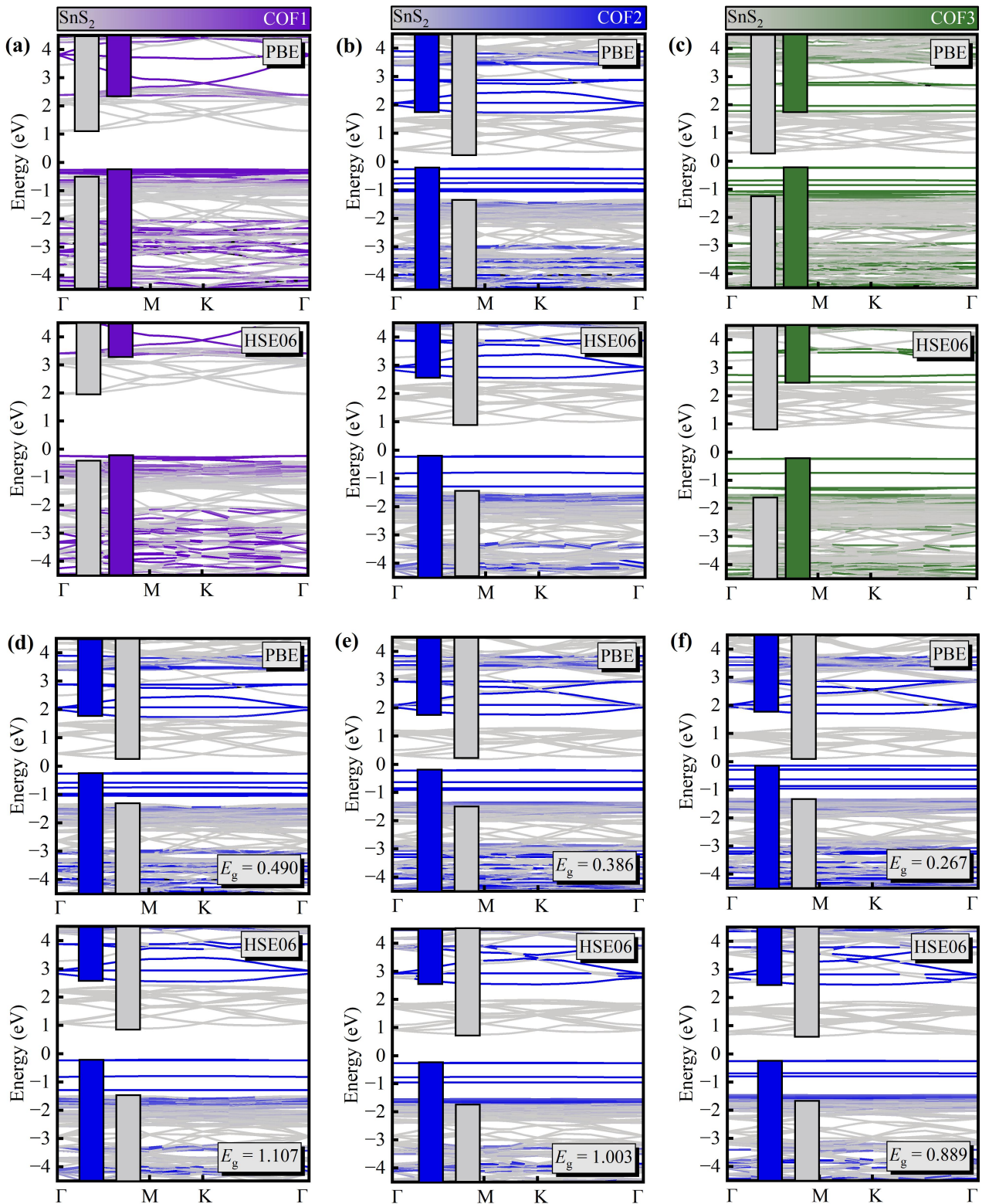


**Fig. S11** Projected band structures of (a) SnS<sub>2</sub>/COF1, (b) SnS<sub>2</sub>/COF2, and (c) SnS<sub>2</sub>/COF3 with PBE and HSE06 methods. Projected band structures of SnS<sub>2</sub>/COF2 under strain (d) 0%, (e) 4%, and (f) 6% with PBE and HSE06 methods. Color bars indicate the band alignments.

## References

1. M. Cao, L. Ni, Z. Wang, J. Liu, Y. Tian, Y. Zhang, X. Wei, T. Guo, J. Fan, and L. Duan, *Appl. Surf. Sci.* 2021, **551**, 149364.
2. X. Jiang, W. Xie, X. Xu, Q. Gao, D. Li, B. Cui, D. Liu, and F. Qu, *Nanoscale* 2022, **14**, 7292–7302.
3. R. Zhang, Y. Zhang, X. Wei, T. Guo, J. Fan, L. Ni, Y. Weng, Z. Zhao, J. Liu, Y. Tian, T. Li, and L. Duan, *Appl. Surf. Sci.* 2020, **528**, 146782.